

An Optically Isolated HV-IGBT Based Mega-Watt Cascade Inverter Building Block for DER Applications

Paul Grems Duncan, Leonard G. Leslie, Jeremy F. Ferrell, W. Lincoln Cornwell, John A. Schroeder¹ — Jih-Sheng (Jason) Lai, Troy Nergaard²

ABSTRACT

High power applications typically use power converters that are large, expensive, are difficult to control, and present significant engineering challenges as power density and power capacity increase. Many thyristor-based systems still exhibit slow switching speeds, have poor reverse bias safe operating area, and/or require high gate currents to remove excess carriers and turn the devices off. These traits constrain their usefulness in high power distributed energy resource applications, especially where higher switching frequencies or compact designs are desired. This paper presents the first optically isolated high-power cascaded inverter based upon recent advances in optical current and voltage sensors, optical interconnects, and High-Voltage Integrated Gate Bipolar Transistors (HV-IGBTs). Development of stackable topologies enables extremely high power systems to be realized, and when combined with optical voltage and current sensors as well as optical control interfaces, enables a topology that tremendously simplifies development within the high-power electronics environment. The modularized HV-IGBT inverter offers tangible benefits over conventional thyristor-based inverters and is specifically targeted for distributed energy resource applications. Results concerning cost-benefit analysis in areas including efficiency improvement, reliability improvement, cost reduction, as well as size and weight reduction will be presented. Additionally, the status and performance of the system will be outlined, including design parameters concerning maximum voltages, currents, harmonics, switching frequencies, as well as performance of the optical communication/sensory subsystems.

1. INTRODUCTION

This research effort has targeted issues that are impeding state-of-the-art, next-generation advances in power conversion technologies, specifically, the problems associated with existing thyristor-based, multilevel converter systems and how they are applied to distributed energy resource (DER) applications. State-of-the-art converters have severe limitations due to one or more of the following:

- Slow switching speeds requires larger-sized passive components (a power density and cost problem),
- The reverse bias safe operating area (RBSOA) of most thyristor-based devices is small (a design constraint),
- When turning off the opposite-side anti-parallel diode, the main switching devices cannot withstand high rates of current change (di/dt), and the design requires series inductor along with a resistive-diode for current protection as well as some form of a voltage clamp circuit to prevent the device from over voltage failure (over voltage/current as well as cost and efficiency problems),
- The general requirement for shoot-through protection needs a series disconnect switch or fuse between the energy source and the inverter (a failure mode, cost, and layout problem),
- The physical size of existing systems often prevents their wide-scale deployment in space critical applications, such as those on board ship, aircraft, or spacecraft (the power density problem).
- The requirement for external deionized (DI) water-cooling systems to dissipate heat due to switching losses. These systems have high life-cycle maintenance costs and reduce overall system reliability.

The list continues to expand as increasing pressure is placed upon manufacturers to deliver smaller, faster and higher power converters for an ever-growing list of demanding applications. To combat these limitations and to enable the creation of efficient, reliable, high-powered converters, a new generation of power stage technology needs to be developed. Specifically, these power stages are optically interconnected, are based upon the latest IGBT technologies, and use innovative self-contained cooling technologies to provide extremely compact and reliable systems. The advantages of implementing all-optical sensor and feedback schemes, when combined with all-optical gate drive control signals in high-power cascaded inverters are numerous: the high-power output

¹ Airak, Inc., Manassas, VA. Email: pduncan@airak.com

² Center for Power Electronic Systems, Virginia Tech, Blacksburg, VA

stage can be completely isolated from the lower-potential input and control subsystem, resulting in higher reliability, reduced personnel hazard, and simplified gate control implementation.

2. A MULTILEVEL CASCADE INVERTER FOR DER APPLICATIONS

The cascaded multilevel inverter has been recognized as the circuit of choice for DER applications because of its modularity, stackability, and high-quality output waveform. Figure 1(a) shows a three-level cascade inverter circuit topology using three full-bridge inverters. With additional full-bridge inverter sets stacking for individual phases, a higher-level inverter can be configured [1]. The output phase-to-neutral and line-to-line voltage waveforms of the three-level inverter are shown in Figure 1(b).

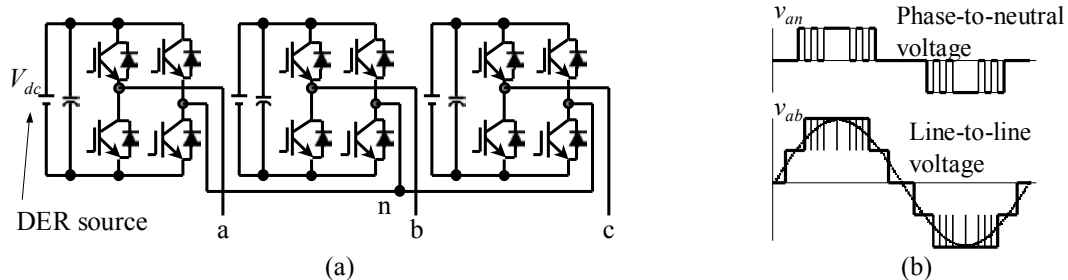


Figure 1. A multilevel inverter for DER applications: (a) a three-level cascade inverter; (b) phase and line voltage waveforms.

The HV-IGBT is selected for the inverter because it allows higher switching frequency with voltage and current levels comparable to state-of-the-art thyristor devices. To characterize the HG-IGBTs, an optically controlled system was designed and built. The power stage was completely isolated from the control and interface circuits with fiber optic cables. A high-speed digital signal processor (DSP) was programmed to produce the desired pulse-width-modulation and test waveforms. Selected as the device under test (DUT) were Mitsubishi CM1200HB-50H high-voltage insulated-gate-bipolar-transistor (HV-IGBT) modules. Each module contains a pair of IGBTs and diodes, rated at 1200A/2500V full-scale. Considering the thermal management and typical device operating margin requirement, the maximum device test conditions were limited to 700A/2000V.

The HV-IGBT module assembly allows a low-leakage inductance busbar to be used. The main concerns involving high-voltage busbar design are potential insulation breakdown and fire hazard. As a result, the type of the busbar insulation material and the thickness of both insulation material and copper need to be taken into account. The creepage around all screw holes should also comply with Underwriters Laboratories Inc. (UL) standards. In the prototype design, 1/16"-thick Glastik™ material and 3/32"-thick copper sheets were used to construct the entire busbar. They provided sufficient insulation strength and current density, as well as mechanical sturdiness to avoid damage due to heavy cable termination and shipping.

3. GATE DRIVE AND DESATURATION PROTECTION

The gate drive design is the first step to achieving proper HV-IGBT switching. In general, the gate drive resistance should be as small as possible so that the gate current is high enough to increase the switching speed and to reduce the switching losses. The manufacturer of the switches can provide switching loss as a function of the gate resistance, but cannot suggest a proper design value because it is related to the gate drive circuit layout and the associated leakage components. The proposed design takes device gate charge and transconductance characteristic into account to ensure the switching waveform is not noise corrupted.

Desaturation protection is the most advantageous feature that an HV-IGBT has over rival thyristor devices. During testing, a variable voltage was applied across the device to measure the trip-voltage level and determine the desaturation circuit parameters. In the desaturation protection circuit, a set of high voltage diodes and resistors were designed and laid out properly with sufficient spacing requirement to comply with UL standards. After implementing the design, test results indicated that the HV-IGBT tripped at twice the rated current during a short circuit condition. **This implies that the device can prevent short circuit or shoot through failure, which is not possible with other thyristor type devices.**

4. FIBER OPTIC CURRENT SENSOR (FOCS) IMPLEMENTATION

The focus of the fiber optic current sensor has been on the realization of a sensory system that meets the performance specifications of conventional sensors while providing the inherent benefits of optical fiber:

immunity to radiated EMI, electrically non-conductive, intrinsically safe, etc. The world's first quick connect/disconnect current sensor for circular conductors has been developed and successfully applied to the proposed inverter. Figure 2 shows a LEM 1005-T current transformer co-located on the load cable with Airak's FOCS. The LEM CT has a maximum current of 2000A, while the Airak FOCS has been tested to nearly 4000A_{pk-pk}. Installation of Airak's FOCS was literally a snap – the sensor clips onto the load conductor and the fiber cables are dressed to the rear of the signal conditioning equipment. Contrast this with the LEM 1005-T, which requires the rigid conductor be “snaked” through it during installation.

Figure 3 shows the small-signal linearity performance of the FOCS up to 86A RMS. The plot reveals high linearity overall with an R^2 of 0.9972. This includes the deviation that occurs at extremely low currents. Omitting the reading at 1.8A results in an R^2 of 0.9999.

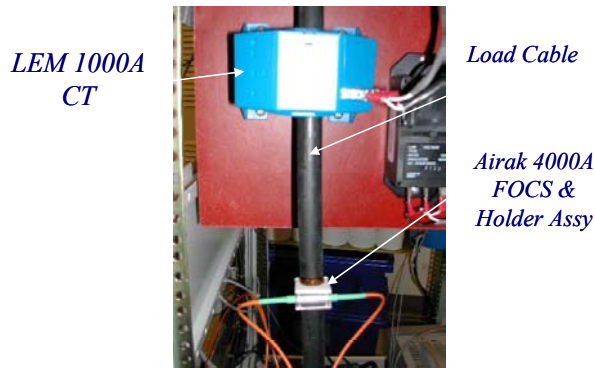


Figure 2. 4000A FOCS installed on the prototype 4/0 AWG load cable, and co-located with the LEM CT to provide correlated measurements.

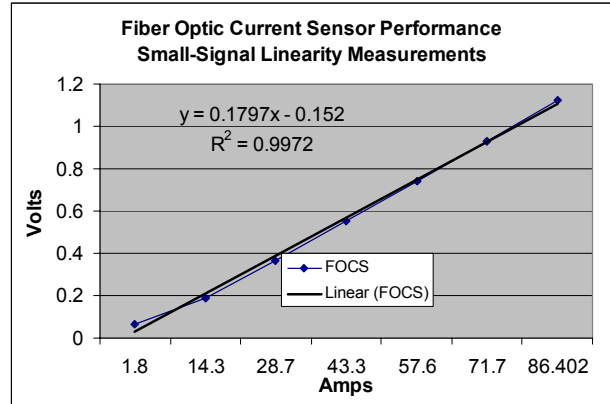


Figure 3. Small-signal linearity measurement of the FOCS. See text for discussion.

5. OPTICALLY ISOLATED FULL-BRIDGE MODULE REALIZATION

As can be seen in Figure 4, the inverter system has been partitioned into three distinct areas: the high-power inverter tray with the integrated optical sensors and optically controlled gate drive, the optical gate interfaces and sensor signal conditioning systems, and the digital signal processing (DSP) computer.

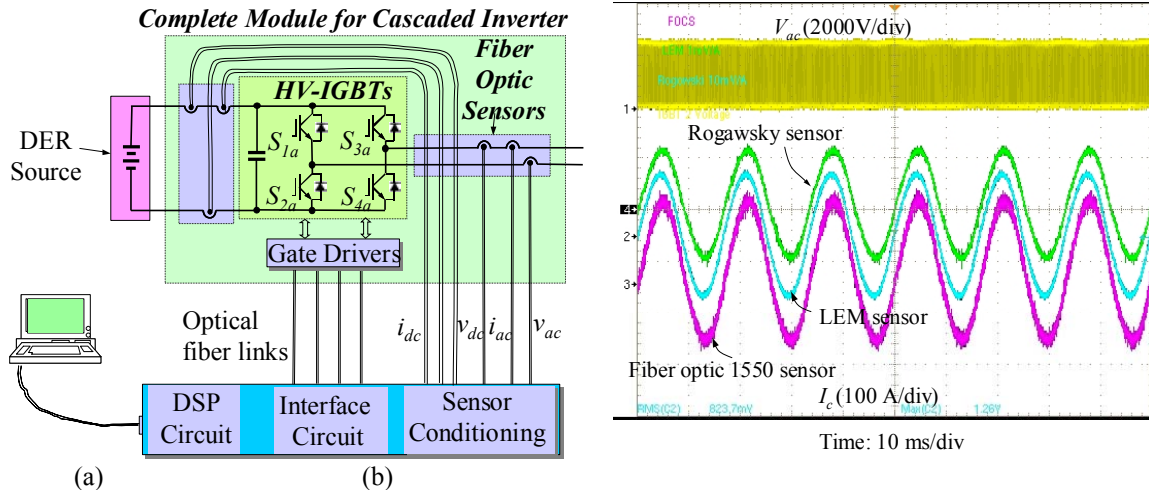


Figure 4. Test setup and output waveform measurement: (a) fully optical isolated inverter module (b) output load current measured with different sensors

In this configuration, there is intrinsic isolation between the high-power tray and the low power interface and signal conditioning equipment due to the non-conducting optical fibers. The initial single-phase prototype program also implemented conventional current, voltage, and temperature sensors for monitoring and

comparative analysis – making the system less robust in terms of safety and overall reliability. Future work will not include any form of conventional current, voltage, or temperature sensors.

6. HV-IGBT SWITCHING VOLTAGE AND CURRENT AND ASSOCIATED ENERGY LOSSES

In order to predict the pulse-width-modulated (PWM) inverter system efficiency, it is necessary to know the device conduction and switching losses. The conduction loss can be obtained from static conducting conditions at different temperatures and can be modeled as a simple voltage source in series with a resistive voltage drop. Although the device switching energy can be obtained from the manufacturer’s datasheet, design and layout variances can introduce substantial performance differences. The device switching energy was determined by integrating the product of the device voltage and current over the entire switching period. Figure 5(a) shows the switching voltage and current along with the corresponding energy waveforms for a measurement at 2000V, 700A; the tests were also conducted at 2000V, 190A as well as 2000V, 370A.

The above switching energy measurement results were curve-fitted into a mathematical model [2]. Using the model, the switching energy at different current conditions was projected, and the inverter PWM switching losses were then calculated based on the switching energy and switching frequency. Figure 5(b) shows turn-on and -off energies obtained from both mathematical model and measurement results. Notice that the curve fitting requires only two points. With three points, it is sufficient to calibrate the mathematical model parameters and to verify the model parameters. Turn-on loss is higher than turn-off loss because the IGBT draws substantial over-current due to the reverse recovery of the opposite side diode. The ratio of E_{on} and E_{off} is around 2:1 in our test. Although E_{on} can be reduced with a lower turn-on resistor R_{g-on} , noise within the circuit could be a major problem if R_{g-on} is further reduced.

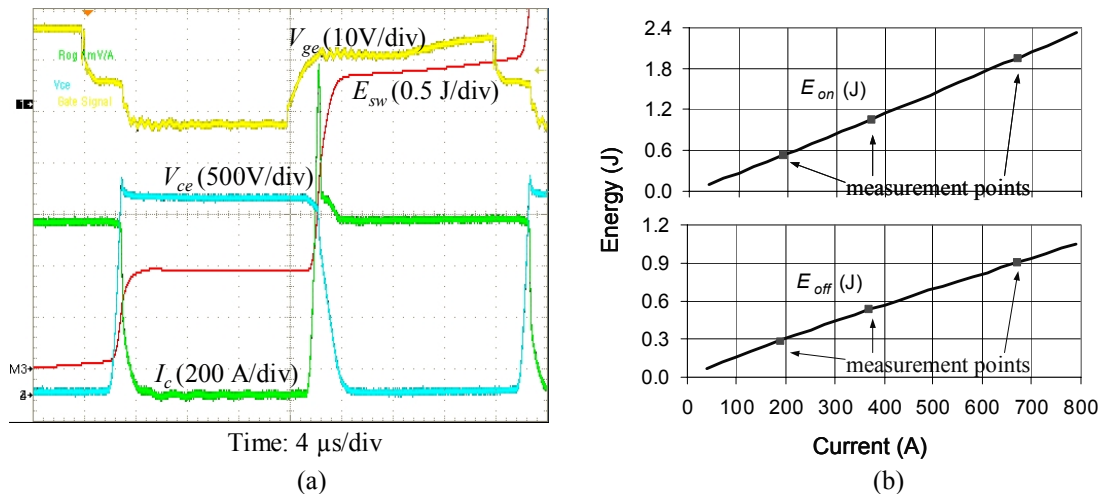


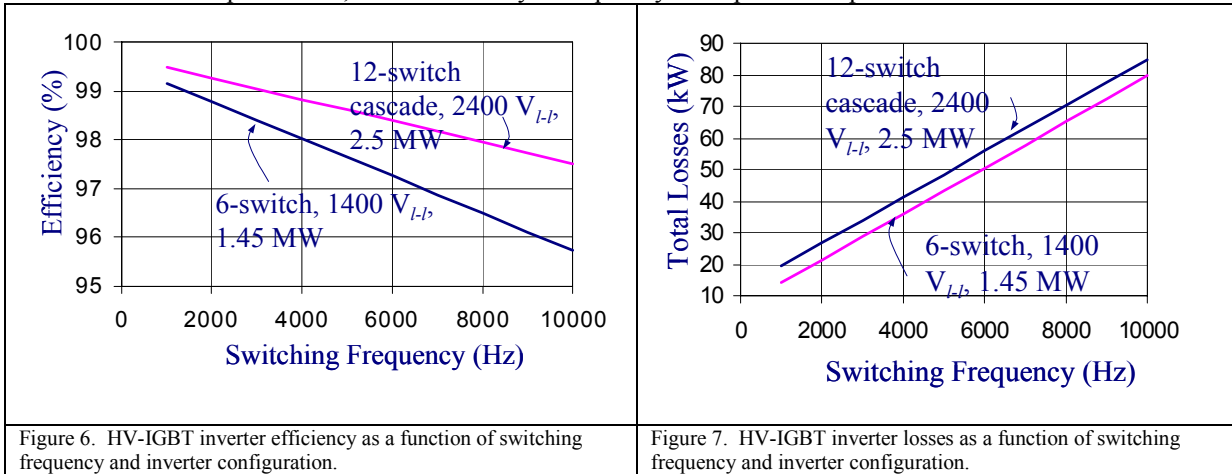
Figure 5. Experimental waveforms: (a) device switching voltage, current, and energy; (b) switching energy model matching over the entire current range.

The DER source voltage level varies among different DER device types. Typically, chemical DER sources such as batteries and fuel cells are low voltage in nature. The voltage obtained from rotational generators can be at a level that is high enough for multi-megawatt systems. Thus, based upon today’s availability, the potential DER sources for the proposed inverter system are microturbines, wind turbines, and small hydro turbines, etc. that produce high voltage outputs through generators. The output voltage level for these turbine generators varies with speed. The maximum DC bus voltage, however, dictates the device voltage rating. Although in the prototype a 2.5 kV device was tested at 2 kV DC bus voltage, it is possible to use 3.3 or 6.6 kV devices to allow higher DC bus voltages. As indicated in Figure 5(a), the turn-off voltage overshoot with our busbar structure has been limited to less than 7.5%. In a typical thyristor based inverter, this number could exceed 50%. Thus, HV-IGBT devices allow the DC bus voltage level to be closer to the rated device voltage level and still have more voltage margin over the thyristor-type devices that require substantial voltage derating. Thus, our voltage and power level selection can simply be based on the device availability.

7. SINUSOIDAL PWM INVERTER EFFICIENCY ESTIMATION

For PWM inverters, the higher switching frequency, the better the output waveform and the smaller the filter size. However, switching loss proportionally increases with switching frequency, and thermal management becomes a major design constraint for high power megawatt level inverters.

Figure 6 shows the HV-IGBT inverter efficiency as a function of switching frequency. As can be seen, the 12-switch cascaded inverter is more efficient than that of a 6-switch system at all relevant switching frequencies, even with a higher system power rating. Although initial component costs will be higher with a 12-switch configuration, over an assumed amortized life cycle of five years and a 0.5% - 1.0% savings in efficiency at a conservative \$0.02 per kW-Hr, the 12-switch system quickly recoups the component cost differential.



The preliminary selection of the DC bus voltage is 2 kV continuous and 2.5 kV peak under regenerated power flow conditions. The device current, although rated at a continuous 1.2 kA, is limited by the thermal/heat removal constraints. The required heat removal capacity for the full-power topology for every four-device bridge is 16.6 kW. Thus if the efficiency can be pushed to 99%, each full-bridge module can be operated at 1.66 MW, and the three-phase, three-level cascaded inverter power level can reach 5 MW.

Figure 7 shows the HV-IGBT inverter system total power losses as a function of switching frequency and inverter configuration. While the losses of a 12-switch system are $\sqrt{3}$ times larger than a comparable-sized 6-switch system, the efficiency of a 12-switch system is much higher. To a limited extent, filter size is inversely related to switching frequency. From a practical point of view, it is easier to fix the size/footprint/ratings of available filter components to the system, then to adjust the switching frequency to optimize losses.

Finally, driving the maximum switching frequency by limiting the acceptable losses within the system is the capacity of the cooling system. Currently, the facilities at CPES/Virginia Tech are limited to sinking no more than 5 kW, which places overall power limitations on the maximum levels that can be tested with the single phase prototype inverter system. Our follow-on future work addresses this specific limitation by moving away from a de-ionized cooling system to an integrated heat pipe configuration that can sink 16.6 kW per full-bridge module, thus enabling higher switching frequencies. According to Figure 7, with the devices used in the single phase prototype system configured as three full-bridge inverter modules and the total output power at 2.5 MW level, the total losses that can be cooled by off-the-shelf heat pipe assemblies indicate that a switching frequency in excess of 5 kHz is possible.

Total system efficiency for a 12-switch system was presented above in Figure 6. Depending upon switching frequency, which is driven in part by the size of the cooling system, Airak's system could be operating within the range of 98.0% to 99.5% efficiency. Although a custom designed heat pipe assembly is possible, we plan to use an off-the-shelf heat pipe that has 8.3-kW cooling capability per two switching devices. Thus, the inverter efficiency will be approximately 99% for a multi-megawatt inverter. If a different controller algorithm is chosen, such as the optimum harmonic elimination method, the efficiency of a 5-MW inverter system could reach 99.5% using cost-effective off-the-shelf cooling devices.

8. TOTAL SYSTEM COST

Establishing a comparative cost basis with respect to MW-level inverters is not a trivial task. Equipment manufacturers are reluctant (at best) to divulge any information concerning the cost of their systems let alone the long-term life-cycle costs associated with operating their systems. Despite this, equivalent systems over 250 kW typically price between \$350/kW to \$1000/kW. Assuming a pre-tax margin of 25% and labor/overhead of 3x direct costs, we have component costs ranging from \$70/kW to about \$200/kW for commercially available systems.

Based upon the experiences involved with building the MW-HV-IGBT inverter system, the total system cost for a scaled, three-phase MW-level prototype system is estimated at \$125K or \$29/kVA. If a labor and overhead assumption of 3x direct costs is assumed, then the system cost is estimated close to \$116/kVA.

9. CONCLUSIONS

The industry's first optically isolated HV-IGBT-based MW-level cascaded inverter building block has been developed. The system uses optical methods to measure output load current (analog signal) as well as provide gate drive (digital signal) control and feedback functions, providing greater reliability, reduced personnel hazard, and simplified gate control implementation. The system successfully demonstrated 1.4 MVA level (2000V, 700A) using 2500 V, 1200 A HV-IGBT devices. A new generation of optical current sensors was performance tested and results indicate equivalent or better performance when compared to standard Rogowski coils. Critical busbar and gate drive design parameters were realized and successfully tested. Performance data concerning system operation was validated and calibrated against established proprietary models, and suggest that the full-12-switch system could operate between 98.0% -- 99.5% efficiency at 2.5 MW using standard PWM control algorithms. It was determined that moving to alternative control algorithms could potentially allow efficiency to remain constant but allow the overall system power to exceed 5 MW with the same or decreased switching losses. The up-front material cost of the HV-IGBT system is approximately 65% of a corresponding equivalent-rated thyristor-based system. Moving to an integrated heat-pipe design represents tremendous life-cycle cost-savings and will be implemented in future work.

REFERENCES

- [1] Jih-Sheng Lai and F. Z. Peng, "Multilevel Converters - A New Breed of Power Converters," *IEEE Transactions on Industry Applications*, May/June 1996, pp. 509–517.
- [2] Jih-Sheng Lai et al., "Efficiency Modeling and Evaluation of a Resonant Snubber Based Soft-Switching Inverter for Motor Drive Applications," in *Conf. Rec. of IEEE PESC*, Atlanta, GA, June 1995, pp. 943–949.